

RESEARCH ARTICLE

Pharmacokinetic properties of newly synthesized retinoid X receptor agonists possessing a 6-[N-ethyl-N-(3-alkoxy-4-isopropylphenyl)amino]nicotinic acid skeleton in rats

Akemi Ogasawara, Yoshiki Murakami, Nobumasa Yakushiji, Fuminori Ohsawa, Jun-ichi Kusaba, Tetsuya Aiba, Yuji Kurosaki, and Hiroki Kakuta

Graduate School of Medicine, Dentistry and Pharmaceutical Sciences, Okayama University, Okayama, Japan

Abstract

Objective: The pharmacokinetic properties of three newly synthesized retinoid X receptor (RXR) agonists were evaluated in rats to elucidate the structural factor influencing their pharmacokinetic properties. **Material and methods:** Three RXR agonists possessing a common 6-[N-ethyl-N-(3-alkoxy-4-isopropylphenyl)amino]nicotinic acid skeleton and side chain structures that are slightly different from each other were prepared as we previously reported (Takamatsu et al., *ChemMedChem*, 2008; 3:780–787). The plasma concentration profiles of these compounds were evaluated following the intravenous and intra-intestinal administrations. Their hepatic metabolism was characterized using rat liver microsomes. **Results:** Based on the plasma concentration profile, NET-3IP (3-isopropoxy) was shown to have a distribution volume of 4.53 L/kg, and to be cleared from the body with an elimination half-time of 0.95 h. The bioavailability of NET-3IP is 16.4%, whereas those of the isobutoxy analog NET-3IB and the cyclopropylmethoxy analog NET-3CPM are 46.5% and 22.6%, respectively. Subsequently, in the experiments using rat liver microsomes, the K_m and V_{max} values of NET-3IP were determined as 7.85 μ M and 0.48 nmol/min/mg protein, respectively. This K_m value is nearly the same as those of NET-3IB and NET-3CPM, but the V_{max} value is noticeably smaller. Additionally, it was revealed that the CYP family mainly metabolizing NET-3IP is different from those metabolizing the other analogs. **Conclusion:** Based on these findings, the pharmacokinetic properties of the compounds possessing this type of the skeleton seem to be largely influenced by a slight modification of the side chain structure.

Keywords: Drug design, structure–property relationship, retinoid X receptor, pharmacokinetics, hepatic metabolism, elimination, disposition, bioavailability

Introduction

Retinoid X receptor (RXR) is a member of the human nuclear receptors, and it functions as an essential partner for other nuclear receptors, such as the retinoic acid receptor (RAR) and the peroxisome proliferator-activated receptor (PPAR)^{1–3}. These receptors are known to form a heterodimer with RXR in a ligand-dependent manner, which then bind to the 5'-upstream regulatory region of the target gene, resulting in the alteration of the transcription process and protein expression^{1–3}. For example, it has been reported that the RAR/RXR heterodimer regulates the expression of a protein called p21, modulating cellular differentiation and proliferation⁴, whereas

the PPAR/RXR heterodimer is involved in the expression of a transporter protein that controls glucose transport into adipose tissues^{5,6}. It is therefore probable that the compounds acting as an agonist to RXR influence various biological functions, and some of them may have a clinically favorable effect on cancer and/or metabolic disorders^{7–10}. In fact, among such compounds, bexarotene (Figure 1A) has been demonstrated to be effective for cutaneous T-cell lymphoma, and it is commercially available in the United States as an approved medicine for lymphoma treatment^{11,12}.

Although bexarotene is clinically valuable, it is known to frequently induce non-negligible adverse

Address for Correspondence: Tetsuya Aiba, Graduate School of Medicine, Dentistry and Pharmaceutical Sciences, Okayama University, 1-1-1 Tsushima-Naka, Okayama 700-8530, Japan. Tel: +81-86-251-8641. Fax: +81-86-251-7926. E-mail: taiba@pharm.okayama-u.ac.jp

(Received 13 September 2010; revised 20 January 2011; accepted 26 January 2011)

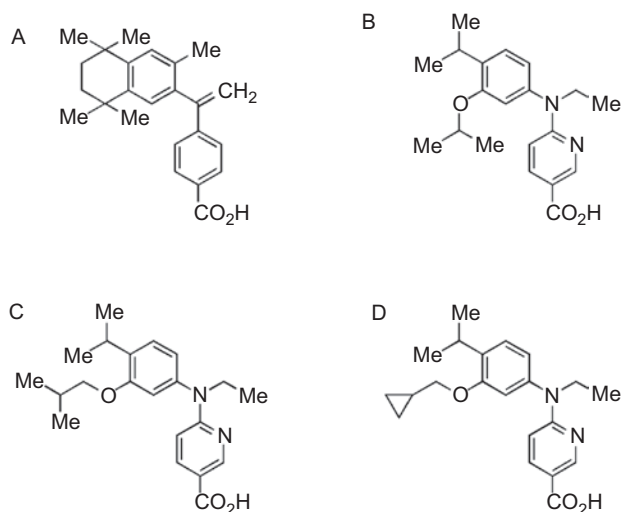


Figure 1. Molecular structures of various retinoid X receptor (RXR) agonists. Keys for the compounds and their molecular weights: (A) bexarotene, 348.48, (B) NEt-3IP, 342.43, (C) NEt-3IB, 356.46, and (D) NEt-3cPM, 354.44.

reactions, including hypertriglyceridemia and hypothyroidism^{13,14}. This is probably due to the fact that bexarotene evenly activates all three RXR subtypes^{1,15,16}, and that RXR subtype γ is involved in the regulation of lipoprotein lipase activity and the serum concentration of thyroid-stimulating hormone^{1,14,17}. Therefore, if a compound that activates RXR subtypes α and β , but not RXR subtype γ , becomes available, it can be used to treat such diseases without unfavorable drug reactions. In addition, bexarotene has a 1,1,4,4-tetramethyltetralin structure, being a highly lipophilic compound with a *ClogP* value, or the calculated logarithm of the octanol/water partition coefficient, of 8.23¹⁶. Considering these in conjunction with the empirical estimation that a compound not exhibiting such a marked lipophilicity becomes a favorable candidate in drug development¹⁸, it has been planned to produce less lipophilic compounds acting as RXR agonists in a subtype-specific manner, and, in fact, as previously reported, one of our compounds, 6-[*N*-ethyl-*N*-(3-isopropoxy-4-isopropylphenyl)amino]nicotinic acid (NEt-3IP, Figure 1B), was shown to have a potent RXR agonistic activity with subtype specificity^{16,19}. This suggests that a further promising drug candidate can be produced as an analogous compound possessing a 6-[*N*-ethyl-*N*-(3-alkoxy-4-isopropylphenyl)amino]nicotinic acid skeleton.

Recently, two analogous compounds of NEt-3IP, 6-[*N*-ethyl-*N*-(3-isobutoxy-4-isopropylphenyl)amino]nicotinic acid (NEt-3IB, Figure 1C) and 6-[*N*-ethyl-*N*-(3-cyclopropylmethoxy-4-isopropylphenyl)amino]nicotinic acid (NEt-3cPM, Figure 1D), became available, and the former was shown to have a more potent agonistic activity than NEt-3IP¹⁹, and their skeletons are the same although their side chain structures are slightly different from that of NEt-3IP. Considering their promising effects as RXR agonists, it seems to be preferable to evaluate their pharmacokinetic properties in the early stage of drug

development, since designing the molecular structure while considering the effect on the compound's pharmacokinetics is important to improve the effectiveness of the drug development process with a reduced risk of its abandonment. This is likely to contribute to cost-effective and time-saving drug development. Therefore, in this study, we characterized the pharmacokinetic properties of these newly synthesized RXR agonists to clarify to what extent structural modification influences their plasma concentration profiles and hepatic elimination processes.

Material and methods

Materials

NEt-3IP, NEt-3IB, and NEt-3cPM were synthesized in our laboratory as previously reported, with a slight modification^{16,19}. Dimethyl sulfoxide (DMSO) and β -NADPH were purchased from Wako Pure Chemicals (Osaka, Japan). Ketoconazole was obtained from Tokyo Chemical Industry (Tokyo, Japan). Quinidine and sulfadimethoxine were purchased from Sigma-Aldrich (St. Louis, MO). All other chemicals used were of the finest grade available.

Animals

Male Wistar rats (200–270 g) were purchased from Japan SLC Inc. (Hamamatsu, Japan). They were housed at 20–25°C and 40–50% humidity with a 12-h light/dark cycle, and were allowed free access to water and a standard diet. All animal experiments were approved by the animal ethics committee of Okayama University and performed in accordance with the guidelines for animal experimentation of the institute.

Evaluation of the plasma concentration profiles of the RXR agonists

After being anesthetized with sodium pentobarbital (50 mg/kg i.p.), each rat was fixed on its back, and the femoral and cervical veins were exposed. For the intravenous administration study, NEt-3IP was dissolved in DMSO at a concentration of 500 mM, and 30 μ L of the solution was infused into the femoral vein for 1 min. Following the infusion, 250 μ L of blood was drawn from the cervical vein at 5, 20, 40, 60, 90, 120, 150, and 180 min using a heparinized test tube. Then, 100 μ L of the plasma specimen was collected following centrifugation at 2000 *g* for 10 min at 4°C for use in analysis. For the intra-intestinal administration study, each rat was fasted overnight prior to the experiment. After the rat was anesthetized and fixed in the same manner as mentioned above, a middle incision was gently made in the abdomen, and the jejunum was exposed. The exposed tissues and bowel were continually moistened with 0.9% sodium chloride solution. The upper part of the intestine was then ligated with surgical silk at two sites: one at the aperture site of the bile duct to close the duct, and the other at a site 10 cm downstream from the first ligation site. After this surgery, 30 μ L of the NEt-3IP DMSO

solution (500 mM) was introduced into the intestine at a site 1 cm downstream from the first ligation site, and blood was drawn in the same manner as described for the intravenous administration study. The plasma concentration profiles of NET-3IB and NET-3cPM were also examined in the same manner as described above.

Evaluation of the hepatic metabolism of RXR agonists

The hepatic metabolism of NET-3IP was evaluated using rat liver microsomes. The microsomes were conventionally prepared from five male Wistar rats (210–250 g) employing a differential centrifugation method^{20,21}. One milliliter of the incubation mixture was prepared based on an isotonic potassium phosphate buffer (pH 7.4) containing 500 µg of the microsomal protein. NET-3IP was dissolved with methanol, and it was mixed with the incubation mixture so as to prepare final concentrations of 0.8, 1.6, 2, 10, and 16 µM. The final methanol concentration in the incubation mixture was 1%²². After a 5-min pre-incubation period, the metabolic reaction was initiated by adding 50 µL of β-NADPH solution to the incubation mixture, and the incubation was carried out for 10 min at 37°C²⁰. The final β-NADPH concentration was set at 1 mM. The metabolic reaction was then terminated by adding and vigorously mixing with 6 mL of ice-cold diethyl ether for the HPLC assay. The elimination rate was calculated based on the difference in the NET-3IP amounts in the incubation mixture before and after incubation. In addition, as a reference study, the elimination rates of nifedipine and propranolol were evaluated in the same manner as described above. Nifedipine was used at concentrations of 2.5, 5, 7.5, 10, and 25 µM. Propranolol was employed at concentrations of 0.06, 0.1, 0.2, and 0.3 µM. Nifedipine and propranolol were arbitrarily selected as representative compounds whose clinical use is common and which are known to be hepatically metabolized. As for the inhibition study, ketoconazole, quinidine, and sulfadimethoxine were chosen as potent inhibitors of CYP3A, CYP2D, and CYP2C, respectively^{23–26}. They were dissolved in the incubation mixture at a concentration at which they could clearly suppress the CYP enzyme activities (40 µM for ketoconazole, 1 mM for quinidine, and 1 mM for sulfadimethoxine)^{23–26}. NET-3IP was used at a final concentration of 2 µM in the inhibition study. Incubation was performed in the same manner as described above. The incubation and inhibition studies were also performed with NET-3IB and NET-3cPM in the same manner as described for those with NET-3IP.

Analytical method

The plasma specimen was first deproteinized by adding 2 mL of 5 mM ammonium acetate (pH 4.7) and 6 mL of diethyl ether. As for the incubation mixture that was already deproteinized with diethyl ether, its aqueous layer was acidified by adding ammonium acetate. The plasma specimen and incubation mixture were then agitated for 5 min, and they were centrifuged at 2000 g for 10 min at 4°C. Then, 5 mL of the organic layer was

transferred to the test tube and evaporated. The residue was reconstituted with 100 µL of methanol, and 25 µL of it was injected into an HPLC equipped with an octadecyl silica column (4 µm, 4.6 × 150 mm, Synergi Fusion-RP®; Phenomenex, Torrance, CA). NET-3IP, NET-3IB, and NET-3cPM were all eluted with a mobile phase consisting of 80% methanol and 20% ammonium acetate (5 mM, pH 4.7). NET-3IP, NET-3IB, and NET-3cPM were spectrophotometrically detected at a wavelength of 278 nm. Their retention times under this HPLC assay condition were 5.0 min for NET-3IP, 6.7 min for NET-3IB, and 5.6 min for NET-3cPM when the mobile phase was used at a flow rate of 1 mL/min. Nifedipine was eluted with a mobile phase consisting of 58% methanol and 42% sodium phosphate buffer (10 mM, pH 2.5), and it was spectrophotometrically detected at a wavelength of 254 nm. Propranolol was eluted with a mobile phase consisting of 43% methanol and 57% sodium phosphate buffer (10 mM, pH 2.5), and it was detected with the spectrofluorometric method at excitation and emission wavelengths of 296 and 353 nm, respectively.

Data analysis

The plasma concentration profile of the RXR agonist observed following intravenous administration was firstly analyzed on the assumption that the profile follows the two-compartment pharmacokinetic model, where the equation described below was employed²⁷:

$$C_{p,iv}(t) = A \cdot e^{-\alpha t} + B \cdot e^{-\beta t} \quad (1)$$

where $C_{p,iv}(t)$ is the plasma concentration of the RXR agonist measured at time t . The parameters α and β denote the rate constants for the distribution and elimination phases, respectively. These rate constants and the parameters A and B are determined in this analysis. The determination was performed with the curve-fitting calculation using the nonlinear least-squares method. Then, the concentration profile of the RXR agonist observed following intra-intestinal administration was analyzed using the two-compartment model accompanied with the first-order absorption process described below²⁷:

$$C_{p,po}(t) = A' \cdot (e^{-\alpha t} - e^{-k_a t}) + B' \cdot (e^{-\beta t} - e^{-k_a t}) \quad (2)$$

$$A' = \frac{k_a}{k_a - \alpha} \cdot A \quad (3)$$

$$B' = \frac{k_a}{k_a - \beta} \cdot B \quad (4)$$

where $C_{p,po}(t)$ is the plasma concentration of the RXR agonist measured at time t , and the parameter k_a denotes the absorption rate constant. With the determined values of the parameters α , β , A , and B , the absorption rate constant k_a is determined with the curve-fitting calculation.

After these determinations, the area under the concentration–time curve (AUC) was calculated as follows:

$$\text{AUC}_{\text{iv}} = \int_0^{\infty} C_{\text{p,iv}}(t) dt \quad (5)$$

$$\text{AUC}_{\text{po}} = \int_0^{\infty} C_{\text{p,po}}(t) dt \quad (6)$$

where AUC_{iv} and AUC_{po} are the AUC values for the plasma concentration profiles following the intravenous and intra-intestinal administrations, respectively. The bioavailability (F) of the RXR agonist is estimated by dividing AUC_{po} by AUC_{iv} , since the dose of the RXR agonist employed in the intravenous study is the same as used in the intra-intestinal study. The apparent volume of distribution at the steady-state ($V_{\text{d,ss}}$) and the elimination half-time ($T_{1/2}\beta$) are calculated employing the following equations:

$$V_{\text{d,ss}} = \frac{D}{\beta \cdot \text{AUC}_{\text{iv}}} \quad (7)$$

$$T_{1/2}\beta = \frac{\ln 2}{\beta} \quad (8)$$

where D is the dose of the RXR agonist, and β is the rate constant mentioned earlier. The natural logarithm of 2 is denoted as $\ln 2$.

Regarding data analysis in *in vitro* experiments, the rates of RXR agonist metabolism measured with the hepatic microsomes were analyzed employing the Eadie–Hofstee equation described below:

$$V = -K_m \cdot \frac{V}{C} + V_{\text{max}} \quad (9)$$

where V is the metabolic velocity for the RXR agonist when it is used at concentration C . The parameters K_m and V_{max} are the apparent Michaelis–Menten constant and the maximum enzyme velocity for metabolism, respectively. The intrinsic clearance was evaluated as V_{max} divided by K_m .

The ClogP value was obtained with ChemDraw® Ultra 7.0 (CambridgeSoft, Cambridge, MA)¹⁶. The ClogP values of NET-3IP, NET-3IB, and NET-3cPM were calculated as 5.61, 6.23, and 5.74, respectively.

Statistical analysis

Data are shown as the mean \pm SE. The significance of differences was evaluated using the Bonferroni t -test, and $P < 0.05$ was considered significant.

Results

Evaluation of the plasma concentration profiles of RXR agonists

The plasma concentration profiles of NET-3IP and its two analogs were firstly evaluated. As shown in Figure 2, their plasma concentrations decreased in a two-exponential manner following intravenous administration. Analysis of their concentration profiles indicated that their apparent elimination half-times are similar to each other, but their volumes of distribution are different, in which the analogous compound NET-3IB exhibits the largest distribution volume out of the three RXR agonists (Table 1). Then, the plasma concentration profile following the intra-intestinal administration was examined with the same dose as employed in the intravenous study being administered (Figure 2). To evaluate the bioavailability, the AUC value was calculated and it was compared with the AUC value calculated in the intravenous study. As a result, it was revealed that NET-3IP shows the lowest bioavailability, whereas NET-3IB exhibits the highest bioavailability (Table 1).

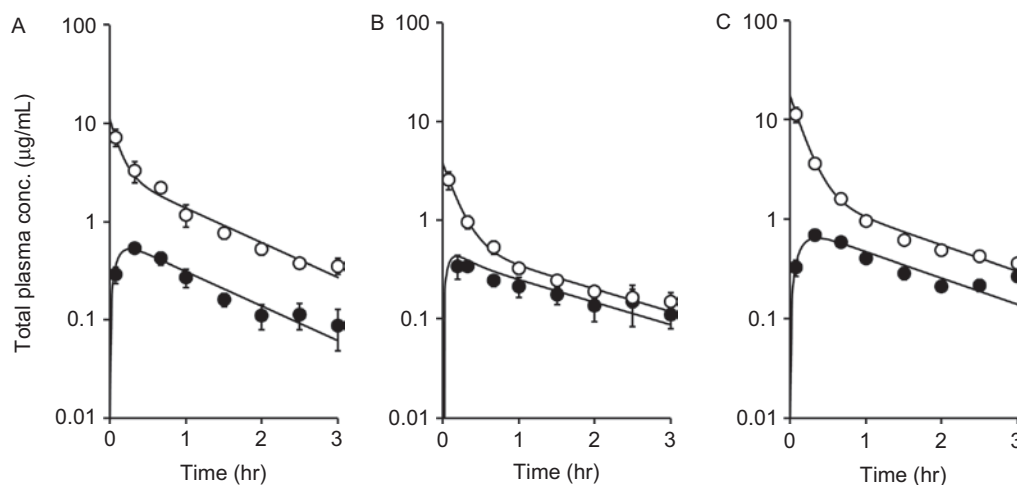


Figure 2. Plasma concentration profiles of the newly synthesized retinoid X receptor (RXR) agonists in rats. The profiles of NET-3IP, NET-3IB, and NET-3cPM are shown in panels (A), (B), and (C), respectively. In each panel, the profile of the RXR agonist observed following intravenous injection is indicated with open symbols, and that observed following intra-intestinal administration is shown with closed ones. The lines are the best-fit lines calculated in the pharmacokinetic analysis. Data are shown as the mean \pm SE of 3–5 experiments.

Evaluation of the hepatic metabolism of RXR agonists

The hepatic metabolic rates of NEt-3IP and its two analogs were examined in the rat liver microsomes. As shown in Figure 3, the slopes generated in the Eadie-Hofstee plot were similar to each other, indicating that the K_m values of these three compounds are also similar. On the other hand, based on the y -intercept of the plot, the V_{max} value of NEt-3IP appeared to be smaller than those for the others. The intrinsic clearances of NEt-3IB and NEt-3cPM were shown to be similar, whereas that of NEt-3IP is one-third of their values (Table 2). The intrinsic clearances of the RXR agonists are noticeably smaller than those of nifedipine and propranolol (Table 2).

Subsequently, an inhibition study was carried out to identify the CYP family mainly contributing to the hepatic metabolism of the RXR agonists in rats. As shown in Figure 4A, the rate of NEt-3IP elimination is markedly suppressed by ketoconazole, but it is less affected by quinidine and sulfadimethoxine. In the case of NEt-3IB, its metabolism is suppressed by ketoconazole and quinidine, but it is relatively unaffected by sulfadimethoxine (Figure 4B). It was also shown that the metabolism of NEt-3cPM is suppressed by all inhibitors, but their suppressive effects seem to be less potent when considering their effects on the metabolism of NEt-3IP and NEt-3IB (Figure 4C).

Discussion

As three newly synthesized RXR agonists possessing a common 6-[N-ethyl-N-(3-alkoxy-4-isopropylphenyl) amino]nicotinic acid skeleton with a side chain structure slightly different from each other recently became available, their pharmacokinetic properties were examined and compared to evaluate to what extent their structural modification influences their plasma concentration profiles and hepatic elimination processes.

As shown in Figure 2, their plasma concentration profiles seem to be similar to each other, although the volume of distribution and extent of bioavailability are largely different. It was calculated that the distribution volume is about 4.5 L/kg for NEt-3IP (Table 1), being the smallest among the three values. This indicates that the distribution property of NEt-3IP is less prominent compared with the others, but it should be noted that its distribution volume is much larger than that of blood vessels, suggesting that these three compounds are largely commonly distributed in the body²⁷⁻²⁹. It was also shown that NEt-3IB has the largest distribution volume (Table 1). Since, based on the $\text{Clog}P$ value, NEt-3IB is considered the most lipophilic compound out of these three compounds, the lipophilicity is probably one of the factors dominating the compound's distribution volume³⁰. Regarding distribution, lipophilic compounds are thought to readily distribute into the central nervous system³¹. In addition, such compounds tend to largely accumulate in adipose tissues, resulting in retardation of the excretion process³¹. Although these distribution and

Table 1. Pharmacokinetic parameters of the newly synthesized retinoid X receptor (RXR) agonists.^a

| RXR agonists | $V_{d,ss}$ (L/kg) | $T_{1/2}\beta$ (h) | F (%) |
|--------------|--------------------|--------------------|-------------------|
| NEt-3IP | 4.53 ± 1.20 | 0.95 ± 0.22 | 16.4 ± 3.82 |
| NEt-3IB | 17.93 ± 2.94^b | 1.34 ± 0.11 | 46.5 ± 7.97^b |
| NEt-3cPM | 5.22 ± 1.81 | 1.33 ± 0.39 | 22.6 ± 1.02 |

^aData are shown as the mean \pm SE of 3–5 experiments.

^b $P < 0.05$: significantly different from the value of NEt-3IP.

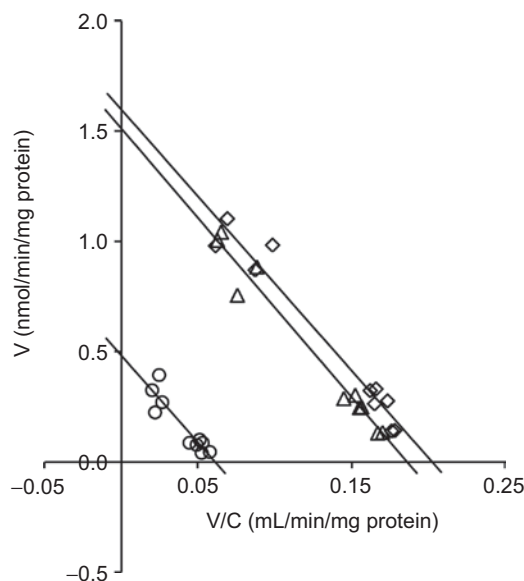


Figure 3. Characterization of the hepatic metabolism of the newly synthesized retinoid X receptor (RXR) agonists. The NADPH-dependent elimination profiles of the RXR agonists evaluated employing rat liver microsomes are shown using an Eadie-Hofstee plot. Each experimental value is presented. The profiles of NEt-3IP, NEt-3IB, and NEt-3cPM are indicated as circles, triangles, and diamonds, respectively.

Table 2. Kinetic parameters of the hepatic metabolism of the retinoid X receptor (RXR) agonists in rat liver microsomes.^a

| Compounds | K_m (μM) | V_{max} (nmol/min/mg protein) | V_{max}/K_m (mL/min/mg protein) |
|---------------------|-------------------------|---------------------------------|-----------------------------------|
| RXR agonists | | | |
| NEt-3IP | 7.85 ± 1.18 | 0.48 ± 0.05 | 0.06 ± 0.01 |
| NEt-3IB | 8.15 ± 0.49 | 1.51 ± 0.06^b | 0.19 ± 0.01^b |
| NEt-3cPM | 7.91 ± 0.60 | 1.60 ± 0.08^b | 0.20 ± 0.02^b |
| Reference compounds | | | |
| Nifedipine | 11.38 ± 0.82 | 4.09 ± 0.18 | 0.36 ± 0.03 |
| Propranolol | 0.21 ± 0.06 | 0.56 ± 0.09 | 2.70 ± 0.87 |

^aParameter values are expressed as the means \pm SE calculated with 10 data points in consideration of error propagation.

^b $P < 0.05$: significantly different from the value of NEt-3IP.

accumulation properties of the newly synthesized RXR agonists were not evaluated in this study, they need to be examined along with adverse reactions caused by these properties in a future study.

Concerning the bioavailability, it was shown to noticeably vary among the compounds (Table 1). In this study, an increased plasma concentration was observed in the late elimination phase of the plasma concentration profile following intra-intestinal administration

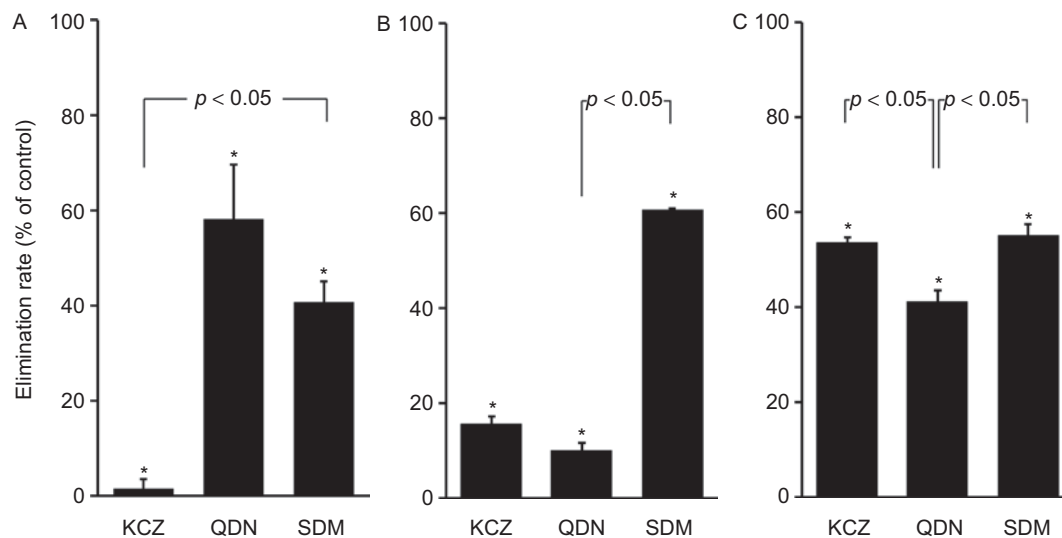


Figure 4. Effects of various CYP inhibitors on the hepatic metabolism of the newly synthesized retinoid X receptor (RXR) agonists. The elimination rates of NEt-3IP, NEt-3IB, and NEt-3cPM measured in the presence of the inhibitor are shown in panels (A), (B), and (C), respectively. Ketoconazole (KCZ), quinidine (QDN), and sulfadimethoxine (SDM) were selected as inhibitors for the rat CYP3A, CYP2D, and CYP2C, respectively, and they were used at concentrations at which they can sufficiently suppress target enzyme activities. Data are shown as the mean \pm SE of 4–5 experiments. * $P < 0.05$; significantly different from the control value (100%).

(Figure 2). This suggests that the plasma concentration profiles of the RXR agonists may not follow the pharmacokinetic model we employed for the analysis. The precise mechanism responsible for the increase is currently unknown, and the bioavailability calculated for each compound may be influenced by the inadequateness of the pharmacokinetic model. However, the finding that NEt-3IP has the lowest and NEt-3IB has the highest bioavailability can be readily accepted when the plasma concentration profiles following the intra-intestinal and intravenous administrations were briefly compared (Figure 2). It is known that a compound's dissolution process in the intestine is often responsible for a difference in bioavailability^{32,33}, but this is unlikely in this case since these compounds are readily dissolved in DMSO and their DMSO solutions were used when they were administered in the intestine. Based on the bioavailability determined with the plasma concentration profiles (Table 1), NEt-3IP seems to undergo extensive first-pass metabolism, whereas NEt-3IB is less metabolized when orally administered. Therefore, to clarify the factors affecting their bioavailability, the hepatic metabolism of these three compounds was then investigated employing rat liver microsomes. As shown in Figure 3 and summarized in Table 2, it was demonstrated that their K_m values are similar, although the V_{max} value depends on the compound and that of NEt-3IP is noticeably smaller than those of the others. In addition, in the inhibition study subsequently performed, it was revealed that the CYP family mainly mediating the hepatic metabolism of those three compounds also depends on the compound (Figure 4). NEt-3IP appears to be mainly metabolized by CYP3A, whereas the metabolism of NEt-3IB is likely to be mediated by both CYP3A and CYP2D. NEt-3cPM seems to

be equally metabolized by CYP3A, CYP2D, and CYP2C families. These may be related to the fact that their side chain structures are slightly different from each other (Figure 1). It is likely that the CYP family commonly recognizes their backbone structure, but the metabolic rate depends on their side chain structure. The side chain structure of NEt-3IP may be preferentially accepted by CYP3A, and the affinity to the CYP2D family can be enhanced by changing the side chain structure from an isopropoxy (NEt-3IP) to isobutoxy (NEt-3IB) moiety. A slight difference in their side chain structures seems to largely influence their affinity for the CYP family. The discrepancy in the CYP families mediating the metabolism observed between NEt-3IP and NEt-3IB resembles that observed between two related antidepressant compounds, imipramine and desipramine (or *N*-demethylated imipramine). The side chain structure of desipramine lacks the methyl group at the tip as compared with that of imipramine. It is known that imipramine is metabolized by both CYP3A and CYP2D, whereas desipramine is solely metabolized by CYP2D³⁴.

As shown in Table 2, the intrinsic clearances of these three compounds are much smaller than those of nifedipine and propranolol, although their bioavailability values are similar to or much larger than that reported for propranolol (Table 1)³⁵. Additionally, the inconsistency in the metabolic properties of NEt-3cPM should be noted. That is, the metabolic profile appears to be similar to that of NEt-3IB (Table 2), but the effects of various inhibitors on its metabolism are clearly different from those of NEt-3IB (Figure 4). These may be explained by assuming that, besides the three CYP families examined, other CYP families, such as CYP1A2, and/or other drug-metabolizing enzymes, such as UDP-

glucuronosyltransferase and *N*-acetyltransferase, are also involved in the metabolic processes^{36–38}, although further investigation is required to fully understand their metabolic processes.

Conclusions

The pharmacokinetic properties of the RXR agonists possessing a 6-[*N*-ethyl-*N*-(3-alkoxy-4-isopropylphenyl) amino]nicotinic acid skeleton are markedly changed by a slight modification of the side chain structure.

Declaration of interest

This work was supported by a Grant-in-Aid for Scientific Research from the Japan Society for the Promotion of Sciences. The authors declare that there are no conflicts of interest associated with the present study.

References

1. Germain P, Chambon P, Eichele G, Evans RM, Lazar MA, Leid M et al. (2006). International Union of Pharmacology. LXIII. Retinoid X receptors. *Pharmacol Rev*, 58:760–772.
2. Giguère V. (1999). Orphan nuclear receptors: from gene to function. *Endocr Rev*, 20:689–725.
3. Mangelsdorf DJ, Thummel C, Beato M, Herrlich P, Schütz G, Umesono K et al. (1995). The nuclear receptor superfamily: the second decade. *Cell*, 83:835–839.
4. Altucci L, Gronemeyer H. (2001). Nuclear receptors in cell life and death. *Trends Endocrinol Metab*, 12:460–468.
5. Shintani M, Nishimura H, Yonemitsu S, Ogawa Y, Hayashi T, Hosoda K et al. (2001). Troglitazone not only increases GLUT4 but also induces its translocation in rat adipocytes. *Diabetes*, 50:2296–2300.
6. Singh Ahuja H, Liu S, Crombie DL, Boehm M, Leibowitz MD, Heyman RA et al. (2001). Differential effects of rexinoids and thiazolidinediones on metabolic gene expression in diabetic rodents. *Mol Pharmacol*, 59:765–773.
7. Bischoff ED, Heyman RA, Lamph WW. (1999). Effect of the retinoid X receptor-selective ligand LGD1069 on mammary carcinoma after tamoxifen failure. *J Natl Cancer Inst*, 91:2118.
8. Leibowitz MD, Ardecky RJ, Boehm MF, Broderick CL, Carfagna MA, Crombie DL et al. (2006). Biological characterization of a heterodimer-selective retinoid X receptor modulator: potential benefits for the treatment of type 2 diabetes. *Endocrinology*, 147:1044–1053.
9. Mukherjee R, Davies PJ, Crombie DL, Bischoff ED, Cesario RM, Jow L et al. (1997). Sensitization of diabetic and obese mice to insulin by retinoid X receptor agonists. *Nature*, 386:407–410.
10. Pinaire JA, Reifel-Miller A. (2007). Therapeutic potential of retinoid x receptor modulators for the treatment of the metabolic syndrome. *PPAR Res*, 2007:94156.
11. Duvic M, Martin AG, Kim Y, Olsen E, Wood GS, Crowley CA et al.; Worldwide Bexarotene Study Group. (2001). Phase 2 and 3 clinical trial of oral bexarotene (Targretin capsules) for the treatment of refractory or persistent early-stage cutaneous T-cell lymphoma. *Arch Dermatol*, 137:581–593.
12. Duvic M, Hymes K, Heald P, Breneman D, Martin AG, Myskowski P et al.; Bexarotene Worldwide Study Group. (2001). Bexarotene is effective and safe for treatment of refractory advanced-stage cutaneous T-cell lymphoma: multinational phase II–III trial results. *J Clin Oncol*, 19:2456–2471.
13. Davies PJ, Berry SA, Shipley GL, Eckel RH, Hennuyer N, Crombie DL et al. (2001). Metabolic effects of rexinoids: tissue-specific regulation of lipoprotein lipase activity. *Mol Pharmacol*, 59:170–176.
14. Sharma V, Hays WR, Wood WM, Pugazhenth U, St Germain DL, Bianco AC et al. (2006). Effects of rexinoids on thyrotrope function and the hypothalamic-pituitary-thyroid axis. *Endocrinology*, 147:1438–1451.
15. Kagechika H, Shudo K. (2005). Synthetic retinoids: recent developments concerning structure and clinical utility. *J Med Chem*, 48:5875–5883.
16. Takamatsu K, Takano A, Yakushiji N, Morishita K, Matsuura N, Makishima M et al. (2008). Reduction of lipophilicity at the lipophilic domain of RXR agonists enables production of subtype preference: RXR α -preferential agonist possessing a sulfonamide moiety. *ChemMedChem*, 3:454–460.
17. Haugen BR, Jensen DR, Sharma V, Pulawa LK, Hays WR, Krezel W et al. (2004). Retinoid X receptor gamma-deficient mice have increased skeletal muscle lipoprotein lipase activity and less weight gain when fed a high-fat diet. *Endocrinology*, 145:3679–3685.
18. Lipinski CA, Lombardo F, Dominy BW, Feeney PJ. (2001). Experimental and computational approaches to estimate solubility and permeability in drug discovery and development settings. *Adv Drug Deliv Rev*, 46:3–26.
19. Takamatsu K, Takano A, Yakushiji N, Morohashi K, Morishita K, Matsuura N et al. (2008). The first potent subtype-selective retinoid X receptor (RXR) agonist possessing a 3-isopropoxy-4-isopropylphenylamino moiety, NET-3IP (RXR α /beta-dual agonist). *ChemMedChem*, 3:780–787.
20. Aiba T, Takehara Y, Okuno M, Hashimoto Y. (2003). Poor correlation between intestinal and hepatic metabolic rates of CYP3A4 substrates in rats. *Pharm Res*, 20:745–748.
21. Komura H, Iwaki M. (2005). Pharmacokinetics and metabolism of metoprolol and propranolol in the female DA and female Wistar rat: the female DA rat is not always an animal model for poor metabolizers of CYP2D6. *J Pharm Sci*, 94:397–408.
22. Easterbrook J, Lu C, Sakai Y, Li AP. (2001). Effects of organic solvents on the activities of cytochrome P450 isoforms, UDP-dependent glucuronyl transferase, and phenol sulfotransferase in human hepatocytes. *Drug Metab Dispos*, 29:141–144.
23. Brown HS, Chadwick A, Houston JB. (2007). Use of isolated hepatocyte preparations for cytochrome P450 inhibition studies: comparison with microsomes for K_i determination. *Drug Metab Dispos*, 35:2119–2126.
24. Kobayashi S, Murray S, Watson D, Sesardic D, Davies DS, Boobis AR. (1989). The specificity of inhibition of debrisoquine 4-hydroxylase activity by quinidine and quinine in the rat is the inverse of that in man. *Biochem Pharmacol*, 38:2795–2799.
25. Kotegawa T, Laurijssens BE, Von Moltke LL, Cotreau MM, Perloff MD, Venkatakrishnan K et al. (2002). *In vitro*, pharmacokinetic, and pharmacodynamic interactions of ketoconazole and midazolam in the rat. *J Pharmacol Exp Ther*, 302:1228–1237.
26. Sugita O, Sawada Y, Sugiyama Y, Iga T, Hanano M. (1981). Prediction of drug–drug interaction from *in vitro* plasma protein binding and metabolism. A study of tolbutamide–sulfonamide interaction in rats. *Biochem Pharmacol*, 30:3347–3354.
27. Kato R, Fujiwara A, Kawai T, Moriguchi J, Nakagawa M, Tsukura Y et al. (2008). Changes in digoxin pharmacokinetics treated with lipopolysaccharide in Wistar rats. *Biol Pharm Bull*, 31:1221–1225.
28. Braunschweig J, Stäubli M, Studer H. (1987). Interactions of amiodarone with digoxin in rats. *Br J Pharmacol*, 92:553–559.
29. Davies B, Morris T. (1993). Physiological parameters in laboratory animals and humans. *Pharm Res*, 10:1093–1095.
30. Wilkinson GR. (2001). Pharmacokinetics. In: Hardman JG, Limbird LE, Gilman AG, eds. *The Pharmacological Basis of Therapeutics*, 10th edition. New York: McGraw-Hill, pp. 3–29.
31. Rowland M, Tozer TN. (1995). Distribution. In: Rowland M, Tozer TN, eds. *Clinical Pharmacokinetics*, 3rd edition. Baltimore: Williams & Wilkins, pp. 137–155.

32. Fu LW, Yang LY, Chen WP, Lin CY. (1997). Cyclosporin pharmacokinetics following administration of capsules and Neoral in paediatric patients with lupus nephritis. *Br J Clin Pharmacol*, 44:125-127.
33. Venkataram S, Rogers JA. (1988). Characteristics of drug-phospholipid coprecipitates. II: Bioavailability studies of griseofulvin in rats. *J Pharm Sci*, 77:933-936.
34. Spina E, Avenoso A, Campo GM, Scordo MG, Caputi AP, Perucca E. (1997). Effect of ketoconazole on the pharmacokinetics of imipramine and desipramine in healthy subjects. *Br J Clin Pharmacol*, 43:315-318.
35. Okabe H, Mizukami A, Taguchi M, Aiba T, Yasuhara M, Hashimoto Y. (2003). The increased intestinal absorption rate is responsible for the reduced hepatic first-pass extraction of propranolol in rats with cisplatin-induced renal dysfunction. *J Pharm Pharmacol*, 55:479-486.
36. Fukino K, Sasaki Y, Hirai S, Nakamura T, Hashimoto M, Yamagishi F et al. (2008). Effects of *N*-acetyltransferase 2 (NAT2), CYP2E1 and glutathione-S-transferase (GST) genotypes on the serum concentrations of isoniazid and metabolites in tuberculosis patients. *J Toxicol Sci*, 33:187-195.
37. Vree TB, van den Biggelaar-Martens M, Verwey-van Wissen CP. (1993). Determination of indomethacin, its metabolites and their glucuronides in human plasma and urine by means of direct gradient high-performance liquid chromatographic analysis. Preliminary pharmacokinetics and effect of probenecid. *J Chromatogr*, 616:271-282.
38. Yamazaki H, Komatsu T, Takemoto K, Shimada N, Nakajima M, Yokoi T. (2001). Rat cytochrome p450 1A and 3A enzymes involved in bioactivation of tegafur to 5-fluorouracil and autoinduced by tegafur in liver microsomes. *Drug Metab Dispos*, 29:794-797.